Extending the Concept of Separatrices to QSLs for Magnetic Reconnection

P. Démoulin

Observatoire de Paris, section de Meudon, LESIA, UMR 8109 (CNRS), F-92195 Meudon Cedex, France

Abstract

Magnetic reconnection is usually thought to be linked to the presence of magnetic null points and to be accompanied by the transport of magnetic field lines across separatrices, the set of field lines where the field-line linkage is discontinuous. However, this view is too restrictive taking into account the variety of observed solar flaring configurations. Indeed "quasi-separatrix layers" (QSLs), which are regions where there is a drastic change in field-line linkage, generalize the definition of separatrices. Magnetic reconnection is expected to occur preferentially at QSLs in three-dimensional magnetic configurations.

This paper surveys the evolution of the QSL concept from the beginning to its recent status. The theory was successfully tested with multi-wavelength observations of solar flares. This validates the reconnection scenario as the main physical process at the origin of flares. The confrontation of observations with the state-of-the-art theory gives us also hints how to further develop our understanding of 3-D magnetic reconnection.

Key words: Magnetic Reconnection, Sun: magnetic fields, Sun: X-rays, Sun: flares, Sun: chromosphere

1 Where will magnetic energy release occur ?

The energy needed to power flares is thought to come from the coronal magnetic field, since its free energy dominates over all other forms of stored energy. However, because the coronal plasma has a low resistivity, such energy release is inefficient at the global spatial scales of an active region (AR). For example the energy release is too slow, by more than 10 orders of magnitude for a typical coronal scale-length of 10-100 Mm. Only when small scale lengths are created, the resistive term in the induction equation becomes important and magnetic energy can be released fast enough. Coronal magnetic fields

are forced to evolve continuously by slow photospheric velocities (typically of the order of 0.1 km.s^{-1}, but up to several km.s^{-1} during magnetic flux emergence, compared to a typical Alfvén velocity of 1000 km.s^{-1}). In this context magnetic configurations, where a slow evolution at the boundary leads to the formation of very thin current layers, play a key role.

Magnetic configurations with a complex topology, i.e. with separatrices, are the most obvious configurations where current layers can form both in 2-D and 3-D (Section 2). The concept of separatrices has been generalized in 3-D configurations to QSLs and the theory was successfully tested with multi-wavelength observations of flares and less energetic events (Section 3). Such QSLs are dominantly defined, at a given time, by the photospheric distribution of the magnetic field. QSLs can also be formed by boundary motions which have stagnation points, recent result are reviewed critically in Section 4. Then, I present some perspectives for the development of the QSL theory (Section 5).

2 Magnetic separatrices

The coronal plasma is frozen into the magnetic field almost everywhere, except where current sheets (or layers) can be formed and then dissipated. In particular, current sheets develop along separatrices when the magnetic configuration evolves quasi-statically or dynamically. Separatrices are magnetic surfaces where the magnetic field line linkage is discontinuous (Fig. 1). A particularly important location for reconnection (in a classical view) is the intersection of two separatrices, called the separator.

2.1 Separatrices in magnetic configurations

The simplest example of a magnetic configuration with a complex topology is a 2-D magnetic configuration with an X-point (where the magnetic field vanishes) as in Fig. 1b. Boundary flows invariably lead to the transformation of the X-point into a current sheet when equilibrium configurations are considered (e.g. Sweet, 1958; Low, 1987).

Adding a third perpendicular component of the field, which is invariant in this perpendicular direction (so-called 2.5-D configurations), yields a new possibility for current sheet formation. In 2.5-D current sheets can form along the whole separatrices when shearing flows are present around the photospheric footprint of separatrices (e.g. Zwingmann et al., 1985). This occurs in two distinct cases as follows (Fig. 1). Firstly, when there is an X-point in the poloidal field, as in the 2-D configuration mentioned above (Low and Wolfson,

1988; Finn and Lau, 1991; Vekstein and Priest, 1992). Secondly, when there are field lines tangent to the photospheric boundary (then, they are curved upward, Wolfson, 1989; Low, 1992; Vekstein and Priest, 1992). The general definition of these locations is given by Titov et al. (1993). They called them "bald patches" (BPs) with the visual reference to a haircut (field lines being associated to hairs).

The two cases above have a direct generalization in 3-D magnetic configurations: separatrices are formed by field lines, which thread either null points or bald patches. Current sheets are thought to form along the separatrices when arbitrary foot-point motions are imposed at the photosphere around the separatrices (e.g. Aly, 1990; Lau, 1993).

2.2 Flaring configurations

The initial studies of the topology of flaring configurations have been realized by defining a magnetic field created by discrete sub-photospheric sources. The magnetic null points present between these sources are implicitly at the origin of a complex topology (with intersecting separatrices). Baum and Bratenahl (1980) were the first to calculate numerically the location of intersecting separatrices in a potential configuration formed by four magnetic poles. Indeed, such poles are a good approximation to the field created by subphotospheric elongated flux tubes, that are likely to be present in the convective zone (Démoulin et al., 1994b). Hénoux and Somov (1987) proposed that reconnection along the separator interrupts currents flowing along lines of force releasing the energy stored in these currents. Then, Gorbachev and Somov (1988, 1989) developed the theory and applied it to an observed flare, showing that field lines passing close to the separator connect to the chromospheric flare ribbons. The next logical step, in order to represent the observed photospheric field in a more realistic way, was to introduce many sources (Mandrini et al., 1991, 1993) and to determine their position and intensity by a least-square fitting of the computed magnetic field to the observed one (Démoulin et al., 1994b). In these cases many separatrices are present and the sources should be gathered in groups; that is to say, all the sources used to describe the observed complex shape of one field concentration, like a sunspot, belong to the same group. The connectivity of a field line is then defined by the groups to which the sources, found at both of its ends, belong. This method is called the source method. At first sight, this method seems to depend strongly on the type of sources (poles or dipoles) used in the representation of the field; in fact, even for complex ARs, a pole or dipole representation gives the same topology when the number of sources is large enough to describe well the main polarities of the photospheric magnetogram.

Detailed analyses of various flares using the source method have shown that Hα and UV flare brightenings are located along the intersection of separatrices with the chromosphere; moreover, they are connected by field lines which are expected to form through reconnection in the given configuration (Mandrini et al., 1991, 1993, 1995; Démoulin et al., 1993, 1994b; van Driel-Gesztelyi et al., 1994; Bagalá et al., 1995). These results are valid for a variety of observed magnetic configurations: from quadrupolar ARs to bipolar ones with an S-shaped inversion line. Moreover, when available from transverse field measurements, the photospheric electric currents have been found at the border of the separatrices; they are the source of the free magnetic energy dissipated. These results demonstrate that the location of energy release in flares is defined by the magnetic topology and that the physical mechanism is most plausibly magnetic reconnection.

2.3 Needs for an extended concept

The studied flaring configurations teach us how magnetic reconnection is working in the corona, as follows. For some of the studied ARs we found a magnetic null point in the extrapolated coronal field, mainly when an almost oppositely oriented bipole emerged between the two main polarities of a sunspot group. However, in several ARs no such coronal null point can be linked to the flare, and it is difficult to imagine how a coronal null can exist in any reasonable magnetic configuration associated to the observed photospheric field (Démoulin et al., 1994a). Moreover, the coronal flare is not expected to be linked to the hypothetical nulls which are located at or below the photosphere (in particular around the depth of the sources).

We have also found cases where the energy release location occurred along bald patch separatrices. So far, such cases were found only in small events such as a small flare (Aulanier et al., 1998), in transition region brightenings (Fletcher et al., 2001), in surge ejections (Mandrini et al., 2002), and even as part of the emergence process of an AR (Pariat et al., 2004). Moreover, the theory also predicts the possibility of large scale events (in association with sigmoids, Titov and Démoulin, 1999). The bald patch separatrices for all the studied observed examples was computed using an extrapolation of the photospheric field, while the location of bald patches themselves can be deduced directly from vector magnetograms (with the 180^0 ambiguity resolved).

The computed topology permits to understand the locations of chromospheric and transition region brightenings, flare ribbons and bright loops in all the studied cases, while only part of the studied configurations could be related to magnetic null points or bald patches. These studies indeed teach us that coronal magnetic reconnection occurs in a broader variety of magnetic configu-

rations than traditionally thought. At the same time these studies also clearly show us that the energy release does not involve the entire separatrices, even when a coronal null is present (Hα flare brightenings are present only on a restricted part of the chromospheric footprint of the computed separatrices).

The source method used previously has two main limitations: first, it cannot be used with other extrapolation techniques, because it intrinsically needs sources to define the connectivity and so the separatrices; second, one needs to integrate below the photosphere along a few thousands kilometers, where a magnetic field model is not available. One can overcome the latter difficulty only by setting the point sources at the photospheric level which has the immediate consequence that the observed magnetogram is poorly taken into account (only the total flux and the position of the main polarities are kept). However, this approach has great theoretical advantages since powerful mathematical tools can be used as Longcope and Klapper (2002) demonstrated. They derive an elaborate model of the theoretical configuration defined by the point-like photospheric sources. Such a theoretical configuration has, hopefully, the same basic characteristics as the observed one. However, since the studied magnetic configuration is, by construction, different than the observed one, this does not allow a detailed comparison of the derived topology with the observational evidences of energy release. Furthermore, topologies including magnetic bald patches are naturally excluded in this approach.

There is also a clear theoretical need to generalize the concept of separatrices in 3-D configurations as illustrated in the following basic example. Let's consider a quadrupolar magnetic configuration invariant in one (y) direction as shown in Fig. 1b. The intersecting separatrices define four cells of connectivity. However, when the magnetic configuration has a finite extension in the y direction, in many cases there are no longer separatrices (those without bald patches and with a non-vanishing B_y component, so no magnetic null point). The structural instability of separatrices, when going from 2.5-D to 3-D, was first pointed out by Schindler et al. (1988) in the case of twisted magnetic configurations. However, this structural instability is no longer present when the notion of separatrices is generalized to that of QSLs (Démoulin et al., 1996b). This indeed complements the theory of Schindler et al. by localizing the regions where their enhanced resistivity can occur.

3 Quasi-Separatrix Layers (QSLs)

The analysis of several flaring configurations have shown that the most probable mechanism of energy release is magnetic reconnection. However, both these analyses and theoretical considerations clearly show the need to generalize the conditions in which magnetic reconnection can occur. There have been sev-

eral attempts because the 2-D case is so peculiar that it can be generalized, a priori, in several ways, most of them being incompatible, see e.g. a summary in Démoulin et al. (1996a). The result of the confrontation of theoretical developments with observations have led to the concept of QSLs.

3.1 Definition of QSLs

Magnetic reconnection is most generally defined as the process that cuts and re-assembles magnetic field lines. So let us consider the field lines starting around a point $P(\vec{r})$. An integration over a distance s along (or opposite to) $\vec{B}$ defines the point $P'(\vec{r'})$. At most places, in well behaved 3-D magnetic configurations, a small change of P induces a comparable shift of P'. However, at some special places, and for s large enough, a slight shift of point P induces a drastic change of P' location. In particular cases, P' can shift discontinuously to a new location; such is the case at a separatrix. By extension, a QSL is defined when the shift is drastic. The mapping $\vec{r} \mapsto \vec{r'}$ can be analyzed quantitatively by defining the Jacobian matrix $F = (\partial\vec{r'}/\partial\vec{r})_s$, in particular a QSL is detected by a large norm of F.

For general applications, the dependence of the mapping with s needs to be analyzed; but in solar applications we can restrict, at least in an exploring phase, to a simpler analysis as follows. The photospheric evolution imposes slowly evolving boundary conditions, so the temporal evolution of coronal structures, at least outside flaring times, is much slower than the Alfvén transit time. Then, the most relevant mapping is from one photospheric polarity to the opposite one: $\vec{r}_+(x_+, y_+) \mapsto \vec{r}_-(x_-, y_-)$ and the reversed one $\vec{r}_-(x_-, y_-) \mapsto \vec{r}_+(x_+, y_+)$ which can be represented by some vector functions $(X_-(x_+, y_+), Y_-(x_+, y_+))$ and $(X_+(x_-, y_-), Y_+(x_-, y_-))$, respectively (Fig. 2). The norm $N(\vec{r}_+)$ and $N(\vec{r}_-)$ of the respective Jacobian matrix in cartesian coordinates are:

$$N_\pm \equiv N(x_\pm, y_\pm) = \left[\left(\frac{\partial X_\mp}{\partial x_\pm} \right)^2 + \left(\frac{\partial X_\mp}{\partial y_\pm} \right)^2 + \left(\frac{\partial Y_\mp}{\partial x_\pm} \right)^2 + \left(\frac{\partial Y_\mp}{\partial y_\pm} \right)^2 \right]^{1/2} \quad (1)$$

A QSL was first defined by the condition $N(x_\pm, y_\pm) >> 1$ in both photospheric polarities (Démoulin et al., 1996a; Priest and Démoulin, 1995).

Let us consider a field line linking the photospheric locations (x_+, y_+) to (x_-, y_-) having a normal field component B_{n+} and B_{n-}, respectively. A difficulty with the definition of Eq. (1) is that $N(x_+, y_+) \neq N(x_-, y_-)$ if $B_{n+} \neq B_{n-}$, so that a QSL does not fulfill a unique condition. A better way is to define a function which is independent of the mapping direction such as the

squashing degree Q:

$$Q_+ = \frac{N_+^2}{|B_{n+}/B_{n-}^*|} \qquad \equiv Q_-^* = \frac{N_-^{*2}}{|B_{n-}^*/B_{n+}|}\,, \tag{2}$$

or equivalently

$$Q_- = \frac{N_-^2}{|B_{n-}/B_{n+}^*|} \qquad \equiv Q_+^* = \frac{N_+^{*2}}{|B_{n+}^*/B_{n-}|}\,, \tag{3}$$

where asterisking the functions indicates that their arguments $x_\mp$ and $y_\mp$ are substituted on $X_\mp(x_\pm, y_\pm)$ and $Y_\mp(x_\pm, y_\pm)$, respectively. Then, a QSL is defined by $Q >> 2$ (Titov et al., 2002). A tiny circular region in one polarity is mapped to a very elongated elliptical region in the other polarity inside a QSL. Then Q simply defines the aspect ratio of the ellipse; in other words, how much the initial region is squashed by the field-line mapping.

The QSL-squashing degree Q provides the most important information about the magnetic connectivity. However, it is only part of the whole information provided by the Jacobian matrix, which has four independent parameters. The next most important, after Q, is the expansion-contraction degree $K = \log|\Delta| = \log|B_{n+}/B_{n-}|$ which depends only on the ratio of the normal field components at both photospheric ends of a given field line. It tells us how much the local flux-tube cross section expands or contracts from one boundary to the other. In configurations where B_n is not uniform, it traces the locations of QSLs (e.g. Fig. 5).

3.2 Main properties of QSLs

The main QSL properties, as derived from the analysis of several flares and theoretical configurations, are summarized below.

QSLs include, as a limiting case when $Q \to \infty$, the concept of separatrices (associated both to magnetic null points and bald patches). With separatrices the mapping is so drastic that it is discontinuous.

From a mathematical point of view, a QSL of finite width is not a topological object like a separatrix since this QSL can be removed by suitable continuous deformations of the magnetic field. But in astrophysical plasma like the corona, the same physics is expected to occur at a separatrix and at QSL which is thin enough, as follows. In the framework of ideal MHD, almost any evolution of the magnetic configuration creates an infinitely thin current sheet along a separatrix and a current layer of finite width along a QSL. However, in the

corona local physical processes, like resistivity or kinetic processes, broaden any current region to a finite width. Then, for the physical evolution of coronal fields, there is no basic difference between a separatrix and a QSL provided that the QSL is thinner than the sizes given by the "microscopic" physics. In the case of numerical simulations, no significant difference in the results is expected between a separatrix and a QSL if the QSL is thinner than few grid points since resistivity is adapted to these scales.

The basic magnetic configuration having QSLs in the corona is formed by two interacting magnetic bipoles. When the bipoles are nearly anti-parallel, the configuration has a magnetic null in the corona and a pair of intersecting separatrices (Hénoux and Somov, 1987; Lau, 1993). When the bipoles are slightly less anti-parallel, only QSLs of finite thickness remain (top of Fig. 3). QSLs persist, while becoming thicker, as the two bipoles are becoming more parallel (Fig. 4). In general QSLs are present in most of the 3-D magnetic configurations formed by more than one bipole.

In a configuration formed by two interacting bipoles, the magnetic field line linkage has four basic sets of magnetic connectivities (Fig. 3), just as in 2-D quadrupolar magnetic configurations (Fig. 1). Some configurations have a photospheric magnetogram dominated by two regions: one negative and one positive region; they are called bipolar regions. In such regions the intersection of the QSLs with the boundary is formed only by two extended thin strips (Fig. 3, bottom), one over each magnetic polarity. Two field lines starting nearby on both sides of one strip rapidly diverge in the volume to connect, on the other strip, regions which are very far apart. The way field lines diverge suggests to call the magnetic structure of QSLs a "hyperbolic flux tube" (HFT, Titov et al., 2002). The 3-D shape of this HFT is better understood as one follows its shape from one polarity to the other one (Fig. 5). It starts as an elongated strip over one polarity, then it is transformed progressively to a cross shape in the volume, then it ends to an elongated strip over the other polarity (this strip involved the other branch of the cross). A schema of the cross-section is:

(4)

The QSL shape is robust. For example, the same, simply thinner, shape is found for a larger value of Q in Fig. 5. Also, if we modify the distribution of the magnetic field at the boundary (or the distribution of the electric currents in the volume), the spatial location of QSLs smoothly follow these changes (Fig. 3). This stability of the QSLs comes from their definition: they are derived from the integration of the magnetic field (field lines) and so they are defined by the global properties of the magnetic configuration (rather than by

local ones as for magnetic nulls and bald patches).

The QSL thickness is much more sensitive to modifications of the magnetic configuration than the QSL's shape. For example, the thickness is null with two anti-parallel bipoles, but it increases rapidly as the two bipoles become more parallel (Fig. 4). More generally, the respective locations of the magnetic concentrations at the boundary, but also the importance of the weak magnetic field between them affect strongly the thickness of the QSL (Démoulin and Priest, 1997). The amount of magnetic shear or twist is also important for the QSL thickness. For example, the QSL thickness decreases exponentially with the number of turns (or twist) when this number is typically greater than one (Démoulin et al., 1996b). So, in contrast to the well defined location of QSLs, we can hope, at most, to determine only the order of magnitude of the QSL thickness in coronal configurations.

3.3 Testing the theory with flaring configurations

If QSLs are computed for a coronal configuration, the coronal magnetic field can be determined from the data (photospheric magnetograms) with any relevant model. Since nowadays a non-linear magnetic extrapolation is still a research subject, the coronal magnetic field is usually computed using a linear force-free magnetic field approximation (the current density is proportional to the magnetic field). This mostly restricts the study to magnetic configurations which have a low content of free magnetic energy. This is implies that only relatively small events can be analyzed. One exception is when nearly anti-parallel bipoles interact. In this case the magnetic topology is so strongly defined by the photospheric field distribution that the magnetic shear has a secondary role in defining the QSL locations, so even flares of X class can be successfully analyzed with just a linear force free field (e.g. Gaizauskas et al., 1998). The application of the QSL theory to eruptive flares is presently only limited by our ability to compute very stressed coronal configurations from the observed boundary conditions (vector magnetograms).

When magnetic energy is released in the corona, a significant part of this energy is transported along field lines by thermal conduction fronts and/or energetic particles toward the lower atmosphere. Such energy is detected as Hα and/or UV flare brightenings. For all the flares studied so far, the brightenings are found along, or just nearby, the intersection of QSLs with the chromosphere (e.g. Fig. 6). The brightenings are also connected by magnetic field lines, just as expected by magnetic reconnection theory. Moreover, the QSLs define regions much more restricted in length than the separatrices computed using the source method (Section 2.2), so the QSL theory permits a better determination of the location of magnetic reconnection in the corona (Démoulin

et al., 1997; Mandrini et al., 1997).

The heating of the chromosphere implies a so-called "evaporation" process which produces dense coronal plasma confined to the reconnected loops. The associated X-ray flare loops are observed to link the Hα flare brightenings. These brightenings are also found to be connected by field lines and they are located in the close vicinity of the intersection of the QSLs with the chromosphere (e.g. the pairs on the bottom right panel of Fig. 6, see also Fig. 7). The complementary two sets of field lines are associated to the pre-reconnection field (as shown in the bottom left panel of Fig. 6). The associated loops are not observable most of the time because the coronal plasma is not dense enough due to the low level of heating along these lines. The most frequent case in which pre-reconnection loops can be observed is when an emerging flux is detected in Hα as an arch filament system. A classical example of X-ray observations interpreted with the QSL theory is shown in Fig. 7: the computed field lines, with photospheric foot-points on both sides of QSLs, match the observed chromospheric and coronal structures (arch filament system, XBP and faint X-ray loops, Mandrini et al., 1997).

The flares studied so far show that QSLs are formed in a variety of observed magnetic configurations, ranging from quadrupolar regions (e.g. two nearly anti-parallel bipoles) to bipolar ones (e.g. when the magnetic polarities with like-sign are close by). The bipolar regions include those with an "S"-shaped inversion line (e.g. Fig. 6), as well as those with a nearly potential field and an almost straight inversion line (Démoulin et al., 1997). The quadrupolar case is a direct extension to 3-D of a 2-D magnetic configuration with an X-point (as used in 2-D reconnection models), while the bipolar case is closer, at first sight, to what one might expect for a simple arcade model, but in fact the configuration is not that of a simple arcade model.

3.4 Magnetic energy release in flares

Where does the magnetic energy come from? The magnetic energy available for flaring is associated with non-potential magnetic field and so with the presence of electric currents. Indeed, concentrated electric currents have been found in the studied flares; they are located at the border of the QSLs (see Démoulin et al., 1997; Mandrini et al., 1997, and references therein). Moreover, two current kernels of opposite sign, linked by coronal field lines, are usually present. This indicates that the energy is presumably stored in the magnetic field associated with these field-aligned currents. Two kinds of magnetic field evolution are observed to create these stressed configurations: the most frequent is the emergence of a new magnetic bipole inside a pre-existing one (e.g. Mandrini et al., 1996; Schmieder et al., 1997) while in other cases

photospheric horizontal displacements (without flux emergence) are clearly present (e.g. Gaizauskas et al., 1998).

When does the release of magnetic energy occur? Neither the QSL theory, nor the observations are presently developed enough to answer this question. From the theory one expects that reconnection will occur when the current density become large enough, which can be fulfilled when QSLs become thin enough, but this needs to be quantified. From the observations we cannot deduce the time evolution of the coronal magnetic configuration, since the numerical techniques to compute the coronal field are too limited. Nevertheless, a first attempt was made to follow the time evolution of QSLs in an X-ray bright point which was interpreted as reconnected loops between emerging and pre-existing fields (Mandrini et al., 1996, Fig. 7). It was found that the calculated QSLs are very thin (typically less than 100 m) during the lifetime of the XBP, but became much thicker ($\geq 10^4$ m) after the XBP has faded as expected by the QSL theory. This kind of study needs to be repeated when Solar B data becomes available.

Energy release at some QSLs can also be stimulated by the nearby reconfiguration of the magnetic region due to reconnection. This process, called "sympathetic flaring", occurs when one flare is triggered by another. Three examples of such flares were studied by Bagalá et al. (2000). In each case the Hα brightenings and X-ray loops were found to be associated with QSLs just as in the previous studies (see Démoulin et al., 1997; Mandrini et al., 1997, and references therein). The observations show that each flare stimulates energy release in spatially separated QSLs, creating the "sympathetic flaring".

3.5 Using QSL theory to understand complex cases

After testing the QSL theory in several simple configurations, where two interacting bipoles could clearly be identified, the theory has since been used to understand more complex cases. One example is a sub-flare which apparently had only one X-ray loop along the inversion line of the photospheric field (Schmieder et al., 1997). The Hα ribbons had also an unusual "fork-shaped" spatial organization. However, the computation of the coronal field and the associated QSLs allowed us to understand the multi-wavelength observations of this flare in the classical framework of an emerging bipole interacting with the pre-existing coronal magnetic field. The geometry of the emergence created a peculiar QSL organization which was reflected in the appearance of the Hα ribbons. The apparent X-ray loop was found to be indeed the superposition of the two sets of unresolved reconnected loops.

Another study of energy release in a complex magnetic configuration was asso-

ciated with transition region brightenings (Fletcher et al., 2001). The hot coronal loops were found to extend along the computed QSLs, while the transition region brightenings were found close to the QSL intersections with the photosphere. Furthermore, they found that the element abundance of the brightenings depends on the type of topological structure present. The brightenings associated with "bald patch" separatrices (a subset of QSLs) had abundances closer to photospheric values, while those associated with other QSLs had abundances closer to coronal values. The difference was associated with the different atmospheric height at which magnetic reconnection occurs (i.e. chromosphere or corona).

QSLs are also expected to play a key role in the very small events that contribute to coronal heating. Because most of the photospheric magnetic flux is confined to thin flux tubes, very thin QSLs are present in the corona with a thickness much smaller than the flux tube size. Démoulin and Priest (1997) have suggested that turbulent resistivity may be triggered in a QSL. Once this happens the QSL rapidly evolves into a dynamic current layer that releases energy by fast reconnection at a rate that they estimated to be sufficient to heat the corona. However, testing precisely the role of QSLs in small scale events is limited by both the spatial resolution and the sensitivity of the instruments. Nevertheless, a correlation between the Hα and the soft X-ray emissions of an AR with the computed QSLs was successfully found outside flaring times by Wang et al. (2000).

QSLs are also a key to understand the localization of energy release in larger scale configurations such as partial reconnection between two ARs. When sufficient plasma density is present in, at least, one of the reconnected loops, this can lead to the sudden appearance of interconnecting arcs. An example of such interconnecting arcs was found in association with "bald patch" separatrices by Delannée and Aulanier (1999). In the case studied by Bagalá et al. (2000), the X-ray arc was associated with QSLs just as it would be for a normal flare loop (Fig. 8). First reconnection is driven "quietly" by the rotation of one of the involved ARs; then, "dynamically" by a flare in the other AR.

The above results give us some confidence on the development of 3-D magnetic reconnection involving QSLs. They show that one needs to go beyond the classical generalization of 2-D magnetic null points, and associated separatrices, to 3-D. Magnetic reconnection occurs under more general circumstances when small scale lengths are formed in the system at the locations where a drastic change in the field line linkage is present.

4 Link between QSLs and stagnation-type flows

4.1 Brief summary on the effects of stagnation-type flows

Stagnation-type flows, which are defined as having a null velocity at one or more points, have a local stream-line topology that is equivalent to the topology of field lines around an X-type magnetic null. A basic incompressible 2-D stagnation-type flow is:

$$\vec{v} = \frac{V}{l_{sh}}(y, x)\,. \tag{5}$$

Using the frame transformation $(x', y') = (x + y, x - y)/\sqrt{2}$, rotated by $\pi/4$ with respect to the frame (x, y), the equations of stream lines are:

$$x' = x'_0 \exp\left(\frac{V}{l_{sh}}t\right) \quad ; \quad y' = y'_0 \exp\left(-\frac{V}{l_{sh}}t\right)\,. \tag{6}$$

So the flow introduces a large distortion to the initial plasma distribution for $t \gtrsim l_{sh}/V$; in particular, it brings plasma elements, which where initially well separated (around the axis $x' = 0$), close together (around the axis $y' = 0$). Applied as a boundary condition to a magnetic field, this kind of flow is then expected to create a large differential magnetic shear, and so to generate a strong current layer, around $y' = 0$.

The formation of strong current layers associated to stagnation-type flows is demonstrated by MHD simulations (Longcope and Strauss, 1994; Milano et al., 1999). Vortex flows are imposed at the boundary on an initially uniform field. Subsequently, a current layer starts to form in the volume due to the stagnation-type flow present in between two vortices, and later the current in this layer is amplified by the mutual attraction of the two twisted flux tubes (formed by the vortices). Longcope and Strauss (1994) clearly showed how this type of flows leads to a very strong deformation of the initially simple field-line connectivity (indeed these flows create QSLs). They also found current layers which are formed with a thickness that decreases exponentially with time, implying an exponential growth of the current density.

4.2 Analytical developments

Titov et al. (2003) studied the evolution of a magnetic field between two planar boundaries (located at $z = \pm L$) where the flows are:

$\vec{v}(z = -L) = V_s \tanh(y/l_{sh})\hat{x}$, $\vec{v}(z = L) = V_s \tanh(x/l_{sh})\hat{y}$, and l_{sh} is a "photospheric" scale length. They assumed that these boundary flows extended linearly in the volume ($-L < z < L$), so the velocity can be written as:

$$\vec{v}(x, y, z) = \frac{V_s}{2}\left[\left(1 - \frac{z}{L}\right)\tanh\left(\frac{y}{l_{sh}}\right)\hat{x} + \left(1 + \frac{z}{L}\right)\tanh\left(\frac{x}{l_{sh}}\right)\hat{y}\right] . \qquad (7)$$

This gives a stagnation-type flow in the middle plane ($z = 0$): $\vec{v}(x, y, 0) = V_s/2\,(\tanh(y/l_{sh})\hat{x} + \tanh(x/l_{sh})\hat{y})$, which reduces to Eq. (5) for $x, y << l_{sh}$ ($V = V_s/2$). It has the advantage of being bounded by $V_s/\sqrt{2}$ for $|x|, |y| >> 1$. Titov et al. (2003) derived the analytical expressions for the mapping of $x(t), y(t)$ to the initial positions $x(0), y(0)$ at $z = 0$. These expressions show that the strong mapping distortion is limited to a thin layer around the $x = y$ line. This layer has a thickness exponentially decreasing with time ($\approx 2\sqrt{2}e^{-(V_s t/2l_{sh})}l_{sh}$) while its length is finite ($\approx 2.5 l_{sh}$). The maximum squashing degree, located at $x = y = 0$, is $Q_{\mathrm{v,max}} = 2\cosh(V_s t/l_{sh})$, so it becomes large for times larger than the shearing time l_{sh}/V_s. In short, the imposed flows at the boundary produce a stagnation-type flow in the volume and create QSLs (or equivalently an HFT) together with an associated current layer.

The above evolution assumes that the velocity field of Eq. (7) is induced in the coronal volume by the boundary motions. This is far from being obvious since the corona is dominated by magnetic forces. In fact, the extension of boundary motions into the volume with a linear dependence in z (like in Eq. 7) is known only when the initial field is uniform: $\vec{B} = B_o\hat{z}$ (see e.g. Eq. 11 in Milano et al., 1999). Titov et al. (2003) applied, without justification, the velocity field of Eq. (7) to a magnetic configuration created by four magnetic sources; so, to a configuration where $\vec{B}$ can be strongly non uniform and which had QSLs. Near the axis $x = y = 0$, the field is approximately $(hx, -hy, B_\parallel)$ where both h and $B_\parallel$ are functions of z. Then, they found that the maximum current density (z-component) present at $x = y = 0$, was:

$$\mu_0\, j_{\mathrm{z,max}}(z) \approx 2\left(h + \frac{B_\parallel}{2L}\right)\sinh\left(\frac{V_s t}{l_{sh}}\right) . \qquad (8)$$

Then Titov et al. extended the above kinematic approach to take into account the force balance. The extra magnetic pressure on both sides of the current layer induces a compression of the layer, and thus an amplification of the current. With the force-free condition the current density is multiplied by a factor f (their Eq. 41):

$$f \approx 1 + e^{V_s t/l_{sh}}\left(0.91\frac{h l_{sh}}{B_\parallel} + 0.57\frac{l_{sh}}{L}\right) . \qquad (9)$$

So, with force balance, the current density is amplified with a lower longitudinal field $B_{\|}$ and by a factor growing exponentially with time.

Is the current layer linked to the QSLs of the initial field? The current density both in the kinematic and force free approaches (Eqs. 8 & 9) depends only on the properties of the flow and of the local magnetic field (via h and $B_{\|}$), but **not** on the magnetic mapping between the two boundaries (e.g. as characterized by $Q_{\max} = 2\cosh(2\int_{-L}^{L}(h/B_{\|})dz)$. This is a first indication that the QSLs of the initial field are not linked to the current formation. Moreover, a second indication is that the strongest current layer extends into the middle plane ($z = 0$) along the direction $x = y$, and never along the QSLs of the initial magnetic field (which were along $x = 0$ and $y = 0$). The current layer is more likely to be a direct consequence of the imposed flows, and a similar current layer would probably be present in an initial configuration without QSLs in the vicinity of the stagnation point. For example, let us set $h = 0$, this means that the initial field is uniform and there is no QSL, and, Titov's et al. equations still predict the formation of a similar current layer with $j_{\mathrm{z,max}}$ of comparable magnitude (Eqs. 8 & 9). This is a further indication that the stagnation-type flows, but **not** the QSLs of the initial magnetic field, are responsible for the current layer formation. The currents which are expected to form at the QSLs (see Section 4.4) are not included in this analysis.

More generally, what determines the formation of the current layers? Both the stagnation-type flows and the QSLs of the initial field are important ingredients. Another intrinsic property of an HFT is that it consists of field lines which are "stiff" at the footpoint with strong field and "flexible" at the other footpoint with low field. This is an important approach to further investigate (Titov, 2005).

4.3 Numerical simulations

The numerical experiments of Galsgaard et al. (2003) are in good agreement with the analytical results of Titov et al. (2003). Boundary motions, which induce a stagnation-type flow in the volume, create a concentrated current layer where the maximum current density grows exponentially for $t >> l_{sh}/V_s$ (Eqs. 8 & 9). Both analyses provide a comprehensive description of the mapping distortion and of the current layer generated by a stagnation flow. However, in disagreement with these authors' conclusion, I do not think that this result shows that the formation of current layers at QSLs needs special boundary motions. As we have just noted above, the current layers in this example are not related to the QSLs of the initial magnetic field. Therefore, no general conclusion concerning current sheet formation at the QSLs can be inferred.

The initial magnetic field in the numerical experiments of Galsgaard et al. has very broad QSLs and the mapping distortion, therefore is relatively small initially ($Q_{\max} \approx 40$). These weak initial QSLs are rapidly dominated by the QSLs formed by the imposed flows ($Q_{\mathrm{v,max}}$ reaches $\approx 10^4$ by the end of the simulations, see their Fig. 10). There is no doubt here that the current layers formed by the flows are much stronger than the current layers associated with the initial QSLs. Indeed, as in the analytical example, the current layer is formed around $x = y$, not at the location of the initial QSLs ($x = 0$, $y = 0$).

An important difference between the analytical and numerical cases is that for the latter the magnetic and velocity fields are periodic. This implies the formation of multi-current layers directly associated to the stagnation points. For example their "turn" experiment has a bottom flow shifted by $\delta y = 0.5$, compared to their "twist" experiment, and the resulting currents layers are accordingly shifted by δy. Indeed, I believe that this is true also for any δy with only a modulation of the current by the local magnetic field.

4.4 Why current layers are expected to form at QSLs

A significant difficulty of estimating the current build up at well defined QSLs ($Q >> 2$) is that the magnetic connections of the initial field are highly dependent on their position. In a force-free field, the currents generated by the boundary motions will tend to flow along the field lines of the QSLs. However, in general, the formation of current layers depends on the flow-field within the volume of the corona, but these flows cannot be deduced simply from the boundary conditions. They strongly depend on the magnetic structure of the field, and determining them rigorously is both a non-local and a non-linear problem which is difficult to solve. One still expects the formation of a strong current layer at a QSL from almost any kind of boundary motions overlaying a QSL, because at a QSL, the magnetic stress of very distant regions are brought close together (over the QSL thickness).

One can estimate the maximum current density in an elongated magnetic configuration assuming that field lines stay approximately straight in the central part of the QSLs. Considering a local field (in $-L \leq z \leq L$) approximated as above with $(hx, -hy, B_\parallel)$, independent of z for simplicity, with a boundary flow characterized by an amplitude V_s, and a variation length scale l_{sh}, I get the order of magnitude:

$$\mu_0 j_{\max} \approx \frac{V_s}{2L}\frac{t}{}\frac{B_\parallel}{l_{sh}} e^{2Lh/B_\parallel} \approx \frac{l_{shear}}{2L}\frac{B_\parallel}{l_{sh}}\sqrt{Q_{\max}}\,. \tag{10}$$

This conjecture needs to be tested with numerical simulations.

Initially, the current density is expected to grow linearly with the time t, or equivalently proportionally to the "shearing" distance l_{shear} (Eq. 10). This is the property found by Galsgaard et al. (2003) for their "shear" and "ridged rotation" experiments (their Figs. 7 and 13). Though, these experiments show that current layers do form at the QSLs, the properties of these layers were only marginally analyzed. The authors only reported on the current distribution of their "shear" experiment (their Fig. 6). In this case they found that the current layer is indeed along the QSL and has a thickness compatible with the QSL thickness (≈ 0.2). In the "shear" and "ridged rotation" experiments stagnation flow does not occur, so the association of the current layers with the initially broad QSLs dominates.

A rigorous analysis of the current build up at QSLs has to be done with very thin QSLs because in the corona they are expected to have a significant role only in this case. Re-scaling the numerical box of Galsgaard et al. to a typical AR size, of 100 Mm, gives a QSL thickness in their "shear" experiment of ≈ 20 Mm, which is indeed very large when compared to the thickness found in any flaring configuration. However, equation (10) shows that the current density is expected to grow as $\sqrt{Q_{\max}}$. If the experiments of Galsgaard et al. (2003) would be repeated simply with $Q_{\max}$ larger by a factor 400, then the current density in the QSL would dominate the current density created by the stagnation flows during all of the simulation run. For example, the currents from their "shear" experiment are expected in this case to be 20 times larger than in their Fig. 7. Such experiment would give a QSL thickness ≈ 0.01, or 1 Mm if rescaled to an AR size as above, still a large thickness compared to those found in flaring configurations. Present computer resources are not enough to analyze directly the MHD evolution of QSLs involved in flares and coronal heating since their thicknesses are expected to be of the order of 10^{-3} Mm = 1 km or even lower. Nevertheless, analyzing QSLs with a thickness ≈ 0.1 to 1 Mm, and re-scaling the resistive term, will certainly permit us to better understand their physical properties.

5 Back to developments

A strong step forward in the modelling of the coronal magnetic field, based on photospheric field observations, is needed to understand more deeply how magnetic energy is released. The generalization of separatrices to QSLs was a first step. The application of the developed theory to various observed cases has revealed the strong relationship between plasma observations (e.g. in Hα, UV and soft X-rays) and coronal magnetic configurations. These results demonstrate that flares are coronal events where the release of free magnetic-energy is due to the presence of regions where the magnetic field-line linkage changes drastically. QSL based predictions agree with the observational results of the

Yohkoh satellite, but several open questions remain unsolved (see e.g. Tsuneta, 1997). The QSL results strongly support the hypothesis that 3-D magnetic reconnection is at work in solar flares, and analyses based on QSL theory provide guidelines on the 3-D physics of magnetic reconnection. In particular QSL analysis had broadened our view on the possible magnetic configurations where reconnection can occur.

Even though QSL properties have been analyzed in numerous events, the theory is far from being complete. For example, we are still missing a clear understanding of the current layer development at QSLs even in cases of quasi-static evolution before flaring. Furthermore, we still do not know when magnetic reconnection will start. Does it require the current density to exceed a threshold (e.g. the onset of the ion-acoustic instability) or is the non-linearity of the equations able to induce a stiff increase in the reconnection rate at some point of the evolution?

The theory of QSLs certainly needs to become time-dependent. So far it has been developed for quasi-static configurations, not only because of intrinsic mathematical difficulties, but also because the applications to observations could only be done via magneto-static extrapolations of the photospheric field. This gives the false impression that QSLs are always at a given location in the magnetic configurations, but this is certainly not the case in a reconnecting magnetic configuration, such as occurs in flares. Indeed, as reconnection proceeds, QSLs, just like separatrices, are located along different sets of field lines, and the evolution of the flare ribbons is expected to follow their intersections with the chromosphere.

Another limitation, even more basic than the above time evolution, is the absence of both reliable transverse field measurements and of magnetic extrapolation techniques for strongly sheared (or twisted) magnetic configurations. Presently, QSLs have been analyzed only in analytical 3-D magnetic field models which are simply twisted (Démoulin et al., 1996b). These models predict pairs of J-shaped QSL footprints at the chromospheric level when the configuration has a twist of about one turn. J-shaped Hα ribbons have been observed in several eruptive flares, but the quantitative comparison of the observations to QSLs is waiting for the development of more realistic coronal field computations.

Finally, the development of the QSL theory will allow us to bridge the gap with other approaches and theories. A first step in this direction has been done by Milano et al. (1999). They applied QSL theory to a configuration where MHD turbulence develops. The development of magnetic reconnection at QSLs creates strong shears in the flow, and these generate MHD turbulence causing an efficient cascade of energy to small scales. With larger Lundquist numbers, this turbulence is expected to break any monolithic current layer

into many smaller current layers, so that magnetic reconnection, as well as particle acceleration, will occur at many locations. At this point, MHD will not be able to describe the local processes involved in the reconnection of the thin layers, and kinetic theory will be required. This will be true, not only because the thickness of the layers is considerably smaller than the mean-free path for collisions, but also because the electric fields generated exceed the Dreicer electric field by several orders of magnitude (Priest and Forbes, 2000). Nevertheless, MHD and, in particular, the physics of QSLs will still be useful to determine where these current layers are formed in the large scale magnetic configuration and what the main properties of these layers are.

Acknowledgments:

I thank Cristina Mandrini, Lidia van Driel-Gesztelyi, Slava Titov and the referees for reading carefully, and, so improving the manuscript.

References

Aly, J. J., 1990. Do Current Sheets Necessarily Form in 3D Sheared Magnetic Force-Free Fields ? In: The Dynamic Sun. pp. 176–182.

Aulanier, G., Démoulin, P., Schmieder, B., Fang, C., Tang, Y. H., 1998. Magnetohydrostatic Model of a Bald-Patch Flare. Solar Physics, 183, 369–388.

Bagalá, L. G., Mandrini, C. H., Rovira, M. G., Démoulin, P., 2000. Magnetic reconnection: a common origin for flares and AR interconnecting arcs. A&A, 363, 779–788.

Bagalá, L. G., Mandrini, C. H., Rovira, M. G., Démoulin, P., Hénoux, J. C., 1995. A Topological Approach to Understand a Multiple-Loop Solar Flare. Solar Physics, 161, 103–121.

Baum, P. J., Bratenahl, A., 1980. Flux linkages of bipolar sunspot groups - A computer study. Solar Physics, 67, 245–258.

Démoulin, P., Bagalá, L. G., Mandrini, C. H., Hénoux, J. C., Rovira, M. G., 1997. Quasi-separatrix layers in solar flares. II. Observed magnetic configurations. A&A, 325, 305–317.

Démoulin, P., Hénoux, J. C., Mandrini, C. H., 1994a. Are magnetic null points important in solar flares ? A&A, 285, 1023–1037.

Démoulin, P., Hénoux, J. C., Priest, E. R., Mandrini, C. H., 1996a. Quasi-Separatrix layers in solar flares. I. Method. A&A, 308, 643–655.

Démoulin, P., Mandrini, C. H., Rovira, M. G., Hénoux, J. C., Machado, M. E., 1994b. Interpretation of multiwavelength observations of November 5, 1980 solar flares by the magnetic topology of AR 2766. Solar Physics, 150, 221–243.

Démoulin, P., Priest, E. R., 1997. The Importance of Photospheric Intense Flux Tubes for Coronal Heating. Solar Physics, 175, 123–155.

Démoulin, P., Priest, E. R., Lonie, D. P., 1996b. Three-dimensional magnetic reconnection without null points 2. Application to twisted flux tubes. JGR, 101 (10), 7631–7646.

Démoulin, P., van Driel-Gesztelyi, L., Schmieder, B., Hénoux, J. C., Csepura, G., Hagyard, M. J., 1993. Evidence for magnetic reconnection in solar flares. A&A, 271, 292–307.

Delannée, C., Aulanier, G., 1999. CME Associated with Transequatorial Loops and a Bald Patch Flare. Solar Physics, 190, 107–129.

Finn, J. M., Lau, Y., 1991. Magnetohydrodynamic equilibria in the vicinity of an X-type neutral line specified by footpoint shear. Physics of Fluids B 3, 2675–2683.

Fletcher, L., López Fuentes, M. C., Mandrini, C. H., Schmieder, B., Démoulin, P., Mason, H. E., Young, P. R., Nitta, N., 2001. A Relationship Between Transition Region Brightenings, Abundances, and Magnetic Topology. Solar Physics, 203, 255–287.

Gaizauskas, V., Mandrini, C. H., Démoulin, P., Luoni, M. L., Rovira, M. G., 1998. Interactions between nested sunspots. II. A confined X1 flare in a delta-type sunspot. A&A, 332, 353–366.

Galsgaard, K., Titov, V. S., Neukirch, T., 2003. Magnetic Pinching of Hyperbolic Flux Tubes. II. Dynamic Numerical Model. ApJ, 595, 506–516.

Gorbachev, V. S., Somov, B. V., 1988. Photospheric vortex flows as a cause for two-ribbon flares - A topological model. Solar Physics, 117, 77–88.

Gorbachev, V. S., Somov, B. V., 1989. Solar Flares of 1980 Nov. 5 as the Result of Magnetic Reconnection at a Separator. Soviet Astronomy 33, 57–60.

Hénoux, J. C., Somov, B. V., 1987. Generation and structure of the electric currents in a flaring activity complex. A&A, 185, 306–314.

Lau, Y. T., 1993. Magnetic Nulls and Topology in a Class of Solar Flare Models. Solar Physics, 148, 301–324.

Longcope, D. W., Klapper, I., 2002. A General Theory of Connectivity and Current Sheets in Coronal Magnetic Fields Anchored to Discrete Sources. ApJ, 579, 468–481.

Longcope, D. W., Strauss, H. R., 1994. The form of ideal current layers in line-tied magnetic fields. ApJ, 437, 851–859.

Low, B. C., 1987. Electric current sheet formation in a magnetic field induced by continuous magnetic footpoint displacements. ApJ, 323, 358–367.

Low, B. C., 1992. Formation of electric-current sheets in the magnetostatic atmosphere. A&A, 253, 311–317.

Low, B. C., Wolfson, R., 1988. Spontaneous formation of electric current sheets and the origin of solar flares. ApJ, 324, 574–581.

Mandrini, C. H., Démoulin, P., Bagalá, L. G., van Driel-Gesztelyi, L., Hénoux, J. C., Schmieder, B., Rovira, M. G., 1997. Evidence of Magnetic Reconnection from Hα, Soft X-Ray and Photospheric Magnetic Field Observations. Solar Physics, 174, 229–240.

Mandrini, C. H., Démoulin, P., Hénoux, J. C., Machado, M. E., 1991. Evidence for the interaction of large scale magnetic structures in solar flares. A&A,

250, 541–547.
Mandrini, C. H., Démoulin, P., Rovira, M. G., de La Beaujardiere, J.-F., Hénoux, J. C., 1995. Constraints on flare models set by the active region magnetic topology Magnetic topology of AR 6233. A&A, 303, 927–939.
Mandrini, C. H., Démoulin, P., Schmieder, B., Deng, Y. Y., Rudawy, P., 2002. The role of magnetic bald patches in surges and arch filament systems. A&A, 391, 317–329.
Mandrini, C. H., Démoulin, P., van Driel-Gesztelyi, L., Schmieder, B., Cauzzi, G., Hofmann, A., 1996. 3D Magnetic Reconnection at an X-Ray Bright Point. Solar Physics, 168, 115–133.
Mandrini, C. H., Rovira, M. G., Démoulin, P., Hénoux, J. C., Machado, M. E., Wilkinson, L. K., 1993. Evidence for magnetic reconnection in large-scale magnetic structures in solar flares. A&A, 272, 609–620.
Milano, L. J., Dmitruk, P., Mandrini, C. H., Gómez, D. O., Démoulin, P., 1999. Quasi-Separatrix Layers in a Reduced Magnetohydrodynamic Model of a Coronal Loop. ApJ, 521, 889–897.
Pariat, E., Aulanier, G., Schmieder, B., Georgoulis, M. K., Rust, D. M., Bernasconi, P. N., Oct. 2004. Resistive Emergence of Undulatory Flux Tubes. ApJ, 614, 1099–1112.
Priest, E., Forbes, T., 2000. Magnetic reconnection : MHD theory and applications. Cambridge University Press, Cambridge, UK.
Priest, E. R., Démoulin, P., 1995. Three-dimensional magnetic reconnection without null points. 1. Basic theory of magnetic flipping. JGR, 100 (9), 23443–23464.
Schindler, K., Hesse, M., Birn, J., 1988. General magnetic reconnection, parallel electric fields, and helicity. JGR, 93 (12), 5547–5557.
Schmieder, B., Aulanier, G., Démoulin, P., van Driel-Gesztelyi, L., Roudier, T., Nitta, N., Cauzzi, G., 1997. Magnetic reconnection driven by emergence of sheared magnetic field. A&A, 325, 1213–1225.
Sweet, P. A., 1958. The Neutral Point Theory of Solar Flares. In: IAU Symp. 6: Electromagnetic Phenomena in Cosmical Physics. pp. 123–128.
Titov, V. S., 2005. Pinching of coronal fields. In: Reconnection of Magnetic Fields (eds. J. Birn and E.R. Priest). Cambridge University Press, Cambridge, UK.
Titov, V. S., Démoulin, P., 1999. Basic topology of twisted magnetic configurations in solar flares. A&A, 351, 707–720.
Titov, V. S., Galsgaard, K., Neukirch, T., 2003. Magnetic Pinching of Hyperbolic Flux Tubes. I. Basic Estimations. ApJ, 582, 1172–1189.
Titov, V. S., Hornig, G., Démoulin, P., 2002. Theory of magnetic connectivity in the solar corona. JGR, 107 (8), SSH 3, 1–13.
Titov, V. S., Priest, E. R., Démoulin, P., 1993. Conditions for the appearance of "bald patches" at the solar surface. A&A, 276, 564–570.
Tsuneta, S., 1997. Magnetic Reconnection: Open Issues. In: ASP Conf. Ser. 111: Magnetic Reconnection in the Solar Atmosphere. pp. 409–418.
van Driel-Gesztelyi, L., Hofmann, A., Démoulin, P., Schmieder, B., Csepura,

G., 1994. Relationship between electric currents, photospheric motions, chromospheric activity, and magnetic field topology. Solar Physics, 149, 309–330.

Vekstein, G. E., Priest, E. R., 1992. Magnetohydrodynamic equilibria and cusp formation at an X-type neutral line by footpoint shearing. ApJ, 384, 333–340.

Wang, H., Yan, Y., Sakurai, T., Zhang, M., 2000. Topology of Magnetic Field and Coronal Heating in Solar Active Regions - II. The Role of Quasi-Separatrix Layers. Solar Physics, 197, 263–273.

Wolfson, R., 1989. Current sheet formation in a sheared force-free-magnetic field. ApJ, 344, 471–477.

Zwingmann, W., Schindler, K., Birn, J., 1985. On sheared magnetic field structures containing neutral points. Solar Physics, 99, 133–143.

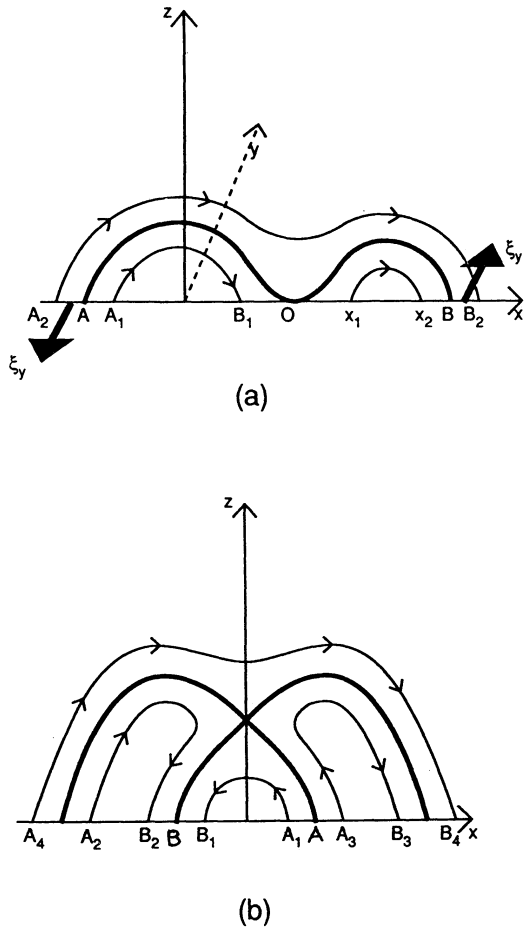

Fig. 1. Basic magnetic topology in a quadrupolar configuration. In (**a**) the separatrix (*thick line*) is tangent to the boundary at the point "O" (a "bald patch"), while in (**b**) two separatrices intercept at an X point. In both cases the connectivity of field lines (*thin lines*) is discontinuous at the separatrices (as emphasized by the labeling of the foot-point of field lines). Shearing photospheric motions (*thick arrows*) induce the formation of a current sheet all along the separatrix in (**a**) (resp. separatrices in (**b**)). (from Vekstein and Priest, 1992).

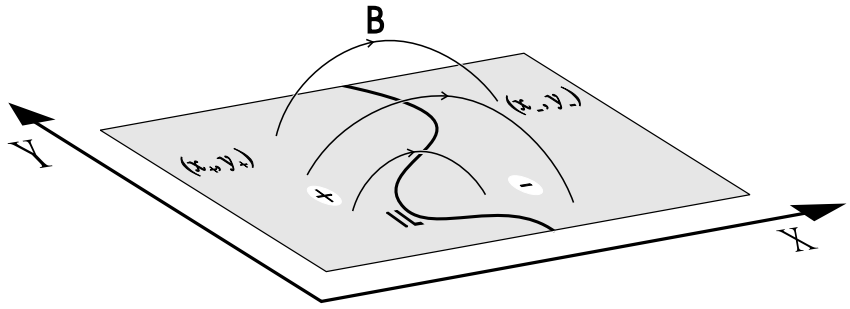

Fig. 2. Schema showing the magnetic connectivity from the photospheric positive polarity (x_+, y_+) to the negative polarity (x_-, y_-). The inversion line (IL) separates the positive and negative polarities (from Titov et al., 2002).

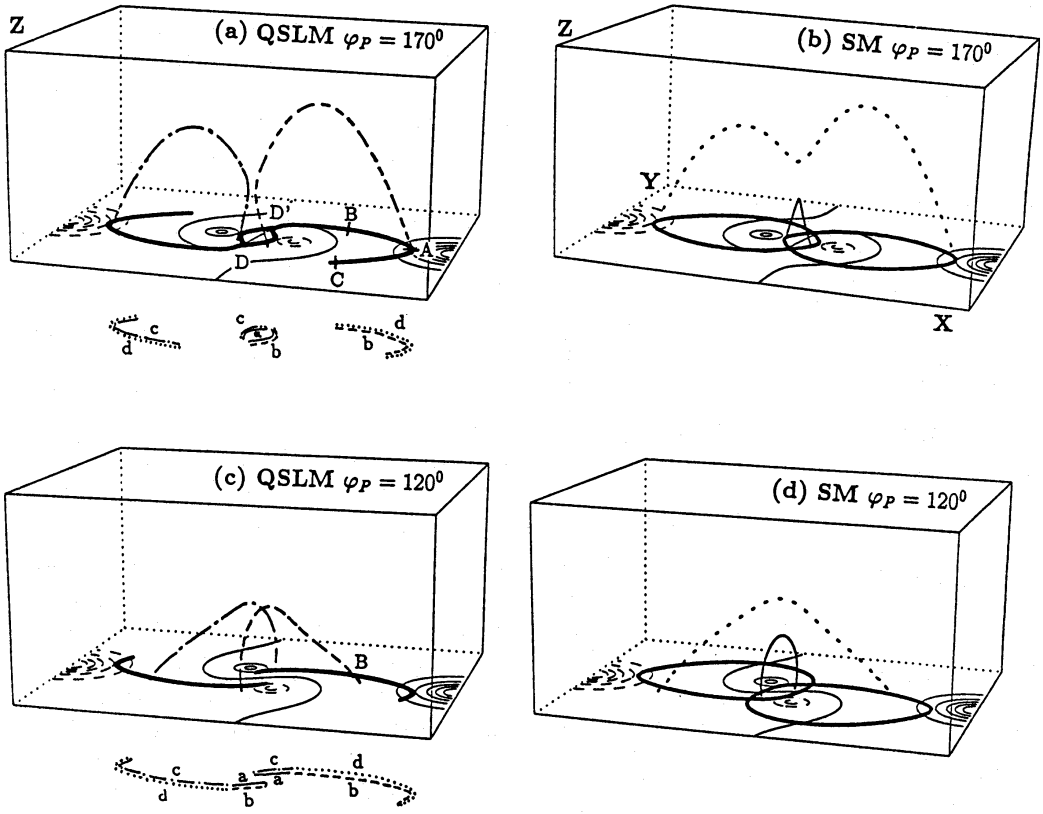

Fig. 3. Magnetic topology of a theoretical magnetic configuration formed by two potential bipoles making an angle φ (the smallest one being inside the largest one). At the lower boundary, the vertical component of the field, B_z, is shown by equi-spaced isocontours with thin continuous (positive), dashed (negative) and thick continuous lines (inversion line of B_z), while the boundary footprint of the QSLs (left panels) and separatrices computed with the source method (right panels) are display with the thickest lines. **(a,b)** $\varphi = 170^0$ (nearly anti-parallel bipoles), **(c,d)** $\varphi = 120^0$. Two pairs of field lines show the typical field-line linkage on both sides of the QSLs. A sketch of the connectivity at the lower boundary has been added with the same convention for line drawing and for field lines; parts linked together have the same lettering (from Démoulin et al. 1996).

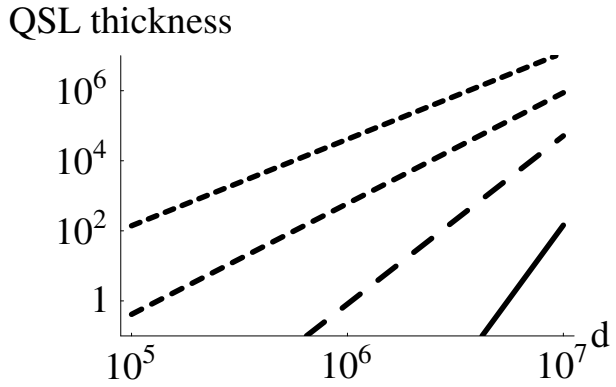

Fig. 4. Dependence of the QSL thickness (in meters) on the depth (d) of the magnetic sources below the boundary for a magnetic configuration formed by two bipoles making an angle φ (see Fig. 3). The size of the main bipole has a typical AR size (10^8 m). From top to bottom the lines are for $\varphi = 10^0, 70^0, 120^0, 150^0$ (for φ closer to 180^0, the theoretical QSL thickness is even lower, becoming null when a null point is present above the boundary, so when separatrices are present). (adapted from Démoulin et al. 1996).

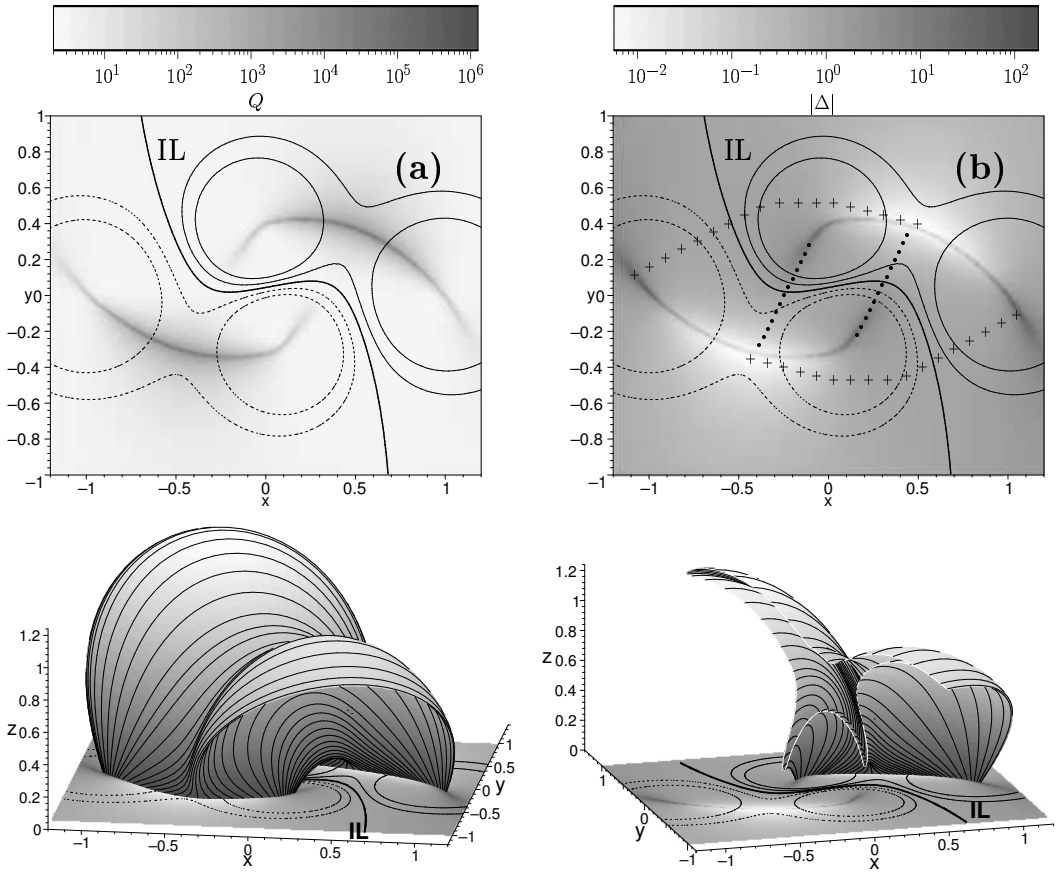

Fig. 5. QSLs of a potential magnetic configuration similar to the lower row of Fig. 3. **Top row**: the photospheric distribution of Q (Eq. 2) and of $|\Delta| = |B_{n+}/B_{n-}|$ superimposed with the magnetogram (B_n being the normal field component at the boundary). The dots and pluses trace the vertical projection of four characteristic coronal flux tubes. **Bottom row**: the QSLs (i.e. HFT) are drawn for the magnetic surface $Q = 100$. In the right panel this surface is cut mid-way to better show the X shape of the QSLs. The important thickness of the QSLs is only due to the low Q value selected for viewing purposes. QSLs in this configuration in fact define a very flat volume, see Fig. 4. In the photospheric plane the distribution of $|\Delta|$ is shown superimposed with the magnetogram (as in the top right panel). (from Titov et al., 2002).

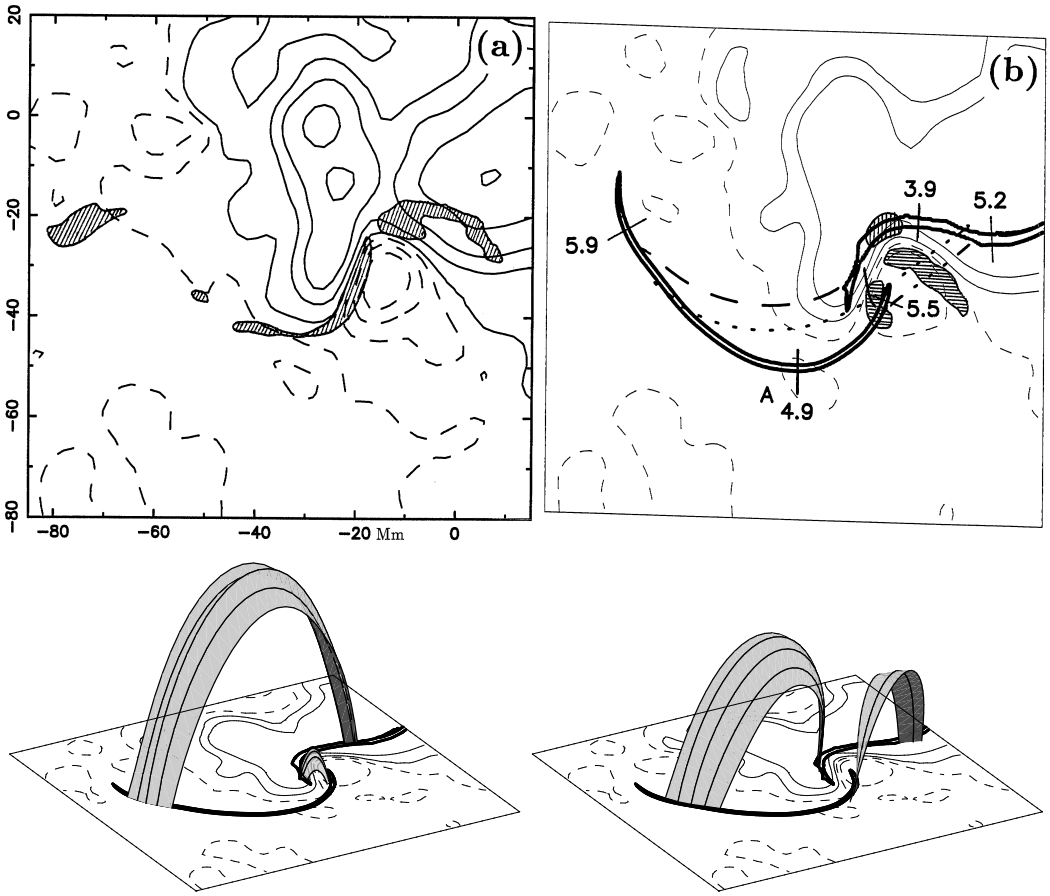

Fig. 6. Example of a flare in a bipolar region where the positive photospheric polarity is simply separated from the negative one with an S-shaped inversion line (AR 2776 on November 5, 1980). The drawing convention is the same as in Fig. 3. **(a)** Observational data: Hα kernels (hatched regions) and isocontours of the longitudinal field B_l. **(b)** Intersection of the QSLs with the photosphere ($N = 10$) for a linear force-free field extrapolation of the longitudinal field. The shaded area represents the locations of observed current regions. The numbers correspond to the decimal logarithm of the QSL thickness (in meters). A few characteristic field lines are shown. **Bottom panels**: perspective views with the typical field lines (drawn as surfaces) on both side of QSLs (from Démoulin et al. 1997).

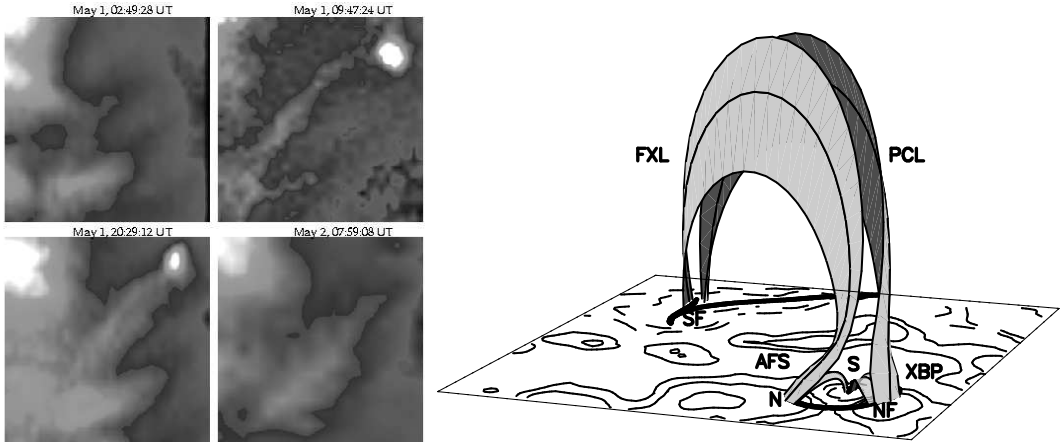

Fig. 7. Example of an X-ray bright point (XBP) observed with SXT/Yohkoh on May 1, 1993. **Left panels**: before (2:49) during (9:47,20:29) and after (7:59) the existence of the XBP. The XBP is the bright, round shaped emission at the top right corner of the images at 9:47 and 20:29 UT. The faint X-ray loop (FXL) is around the first diagonal of the same images. **Right panel**: example of computed field-lines located on the boarders of the QSLs (the QSL footprints are shown with thick lines on top of the magnetogram). The point of view is chosen to better visualize the coronal linkages. The drawing convention is the same as in Fig. 6. The different photospheric field polarities are indicated with letters N, NF, S and SF. The emerging flux, observed as an arch-filament system (AFS) with the polarities N and S, impacts against the pre-existing coronal loops (PCL) connecting the polarities NF and SF. The reconnected field-lines appear as the X-ray bright point (XBP) and the faint X-ray loops (FXL). The three set of observed loops (AFS, XBP, FXL) are found in the computed coronal field. (from Mandrini et al. 1996).

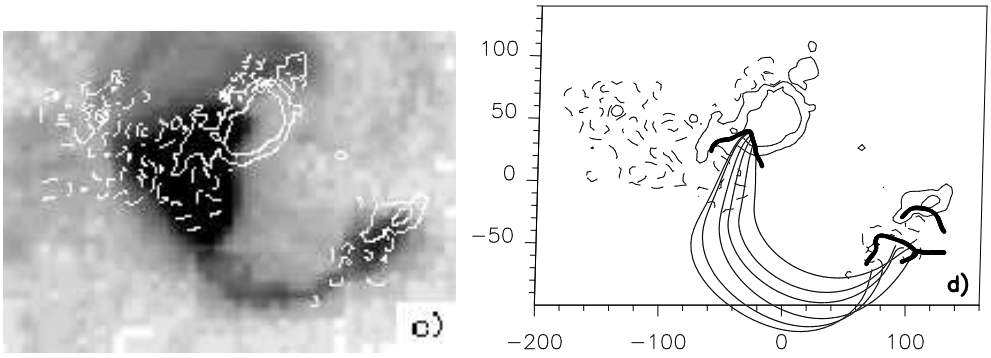

Fig. 8. Example of an interconnecting loop between two active regions (AR 7031 and AR 7038) observed with SXT/Yohkoh on January 30, 1992. **Left panel**: X-ray intensity (reversed contrast) with a co-aligned longitudinal magnetogram (white isocontours) from the Mees Solar Observatory. A flare is present in the top left AR while an interconnecting loop links the two ARs. **Right panel**: the magnetic field model of the two ARs. Characteristics field lines following the shape of the interconnecting arc have been added. These lines have their footpoints at the computed QSLs, which are shown at photospheric level as thick continuous lines. The box axes are labeled in Mm (from Bagalà et al. 2000).